Article

Detecting Exosomes Specifically: A Multiplexed Device based on Alternating Current Electrohydrodynamic Induced Nanoshearing

Ramanathan Vaidyanathan, Maedeh Naghibosadat, Sakandar Rauf, Darren Korbie, Laura G. Carrascosa, Muhammad J. A. Shiddiky, and Matt Trau

Anal. Chem., **Just Accepted Manuscript** • Publication Date (Web): 17 Oct 2014

Detecting Exosomes Specifically: A Multiplexed Device based on Alternating Current Electrohydrodynamic Induced *Nanoshearing*

*Ramanathan Vaidyanathan,‡ Maedeh Naghibosadat,‡ Sakandar Rauf, Darren Korbie, Laura G. Carrascosa, Muhammad J. A. Shiddiky,*and Matt Trau**

Australian Institute for Bioengineering and Nanotechnology (AIBN), Corner College and Cooper Roads (Bldg 75), The University of Queensland, Brisbane QLD 4072, Australia

Tel: +61-7-33464178; Fax: +61-7-33463973

*Email: m.shiddiky@uq.edu.au (MJAS); m.trau@uq.edu.au (MT)

‡ Authors contributed equally

ABSTRACT

Exosomes show promise as non-invasive biomarkers for cancers, but their effective capture and specific detection is a significant challenge. Herein, we report a multiplexed microfluidic device for highly specific capture and detection of multiple exosome targets using a *tunable* alternating current electrohydrodynamic (ac-EHD) methodology - referred to as *nanoshearing*. In our system, electrical body forces generated by ac-EHD act within nanometers of an electrode surface (*i.e.*, within the electrical layer) to generate nanoscaled fluid flow which enhances the specificity of capture and also reduce nonspecific adsorption of weakly bound molecules from the electrode surface. This approach demonstrates the analysis of exosomes derived from cells expressing human epidermal growth factor receptor 2 (HER2) and prostate specific antigen (PSA), and also capable of specifically isolating exosomes from breast cancer patient samples. The device also exhibited a 3-fold enhancement in detection sensitivity in comparison to hydrodynamic flow based assays (LOD 2750 exosomes/μL for ac-EHD *vs* LOD 8300 exosomes/μL for hydrodynamic flow; (n = 3)). We believe this approach can potentially find its relevance as a simple and rapid quantification tool to analyze exosome targets in biological applications.

KEYWORDS

AC electrohydrodynamics, exosomes, multiplex detection, microfluidic devices

INTRODUCTION

Exosomes are membrane nanovesicles released from cells and are present in body fluids such as blood, urine and saliva.[1] They are believed to carry a cargo of proteins, lipids, mRNA, microRNA (miRNA) and transfer this cargo to recipient cells which alter the biochemical composition, signalling pathways, and genomic states of the recipient cells.[2,3] This could also enable them to engage in multiple cell-receptor (surface) interactions simultaneously. Exosomes can thus serve as extracellular messengers mediating cell-cell communication, raising the possibility of these enveloped exosomal receptors in body fluids as novel non-invasive biomarkers for cancer.[3,4] Although their physiological roles are still under investigation there is a growing need for reliable methods for accurate isolation and detection of exosomes from biological fluids. Current methods for the isolation and characterisation of exosomes (*e.g.*, ultracentrifugation, electron microscopy etc.) cannot discriminate between exosomes and other membrane vesicles, lipid structures, or retrovirus particles found in body fluids which are similar in terms of size and density.[4-6] More recently, several microfluidic approaches[7-9] using laminar flow based fluid micromixing have been reported to specifically isolate exosomes from biological fluids. Despite their excellent demonstrations, they are limited by their inability to manipulate surface shear forces to reduce nonspecific adsorption of cells or other molecules and provide quantitative information on these isolated nanovesicles. Therefore, a methodology that can effectively isolate and specifically detect these vesicles and their enveloped biomarkers in complex biological samples could provide further insights into the fundamental role and functions of these poorly understood, yet highly important biological vesicles.

Herein, we present a simple, multiplexed microfluidic platform to address these problems in current exosome detection methodologies. Our approach relies on the use of an alternating current (ac) electrohydrodynamic (ac-EHD) induced surface shear force which

engenders lateral fluid flow within few nanometers of an electrode surface.[10-14] Because this phenomenon involves a shear force within a few nanometers of the surface, we refer to it as *nanoshearing*. When samples containing target exosomes are driven through antibody-functionalized devices under ac-EHD flow (Figure 1), it provides the capability to specifically capture these exosomes by increasing the number of exosome-antibody (surface bound) collisions, which is a result of improved analyte transport. Since the magnitude of this force can be *tuned* externally via the application of frequency and/or amplitude, it can be applied to preferentially select specifically bound exosomes over nonspecifically adsorbed non-target species to surfaces (*i.e.*, non-target species bound weakly to the surface than that of the specifically captured exosomes). This method also provides the capability to simultaneously detect multiple exosome targets using a simple and rapid on-chip naked eye detection readout (*i.e.*, avoids use of any sophisticated instrumental readouts) based on the catalytic oxidation of peroxidase (*e.g.*, from horseradish peroxidise (HRP) conjugated detection antibody) substrate 3,3',5,5'-Tetramethylbenzidine (TMB).[15] Additionally, UV-Visible spectroscopy measurements from the colorimetric solutions provide quantitative analysis of multiple exosomes in a single assay format. The performance of our device for spiked exosome and patient serum samples was comparable with current exosome isolation and detection technologies.

EXPERIMENTAL SECTION

Reagents. Unless stated otherwise, general-use reagents were purchased from Sigma Aldrich (Australia) and immunoassay reagents were obtained from R&D/Life Technologies (Burlington, ON), Thermo-Fisher Scientific (Australia), Abcam (Australia) and Invitrogen (Australia). All reagents and washing solutions used in the experiments were prepared using phosphate buffer saline (PBS, 10 mM, pH 7.4). Stock solutions of antibody were diluted in

PBS. Photoresists for fabrication (Microchem, CA) were used as per manufacturer's instructions.

Design of Multiplexed ac-EHD Devices. In this study, we designed a multiplexed microfluidic device containing asymmetric planar microelectrode pairs within a long microchannel. The device contains three channels with individual inlet and outlet ports with each channel comprising of 50 asymmetric planar electrode pairs (Figure S1, Supporting Information). The small electrode of 50 μm and large electrode of 250 μm are separated by a distance of 50 μm. Adjacent electrode pairs in each segment are separated by a distance of 150 μm. The narrow and wide electrodes of each asymmetric electrode pair in all three channels are connected to individual gold connecting pads (Figure S1, Supporting Information) that form the cathode and anode respectively. The critical gap (r_0) between small (d_1) and large electrodes (d_2) in each pair and the distance between adjacent electrode pairs (r_1) in the array influence the ac-EHD induced fluid flow and the associated micromixing. Previously, Brown et al.[16] and Ramos et al. [17] have demonstrated that the fluid flow rate is inversely proportional to the geometry of the electrodes. The asymmetry in electrode geometry in our device was optimized to engender effective ac-EHD induced fluid flow (*i.e.*, acts as a fluid pump) and micromixing within the channel, and was maintained uniformly throughout each channel as: $r_0/d_2 = 0.2$, $r_1/d_2 = 0.6$, $d_1/d_2 = 0.2$, respectively. The device design was made using Layout Editor (L-edit V15, Tanner research Inc., CA) and written to a chrome mask (5" X 5"; Qingyi Precision Mask-making (Shenzhen) Ltd, China).

Fabrication of Devices. Devices were fabricated at the Queensland node of Australian National Fabrication Facility (Q-ANFF node). Fabrication of the device involves a two-step standard photolithographic process as outlined in Figure S2, Supporting Information.

a. Fabrication of asymmetric gold electrode patterns. Initially, a passivation layer of silicon dioxide (thickness- 300 nm) was deposited on silicon wafers (diameter- 100 mm; thickness-1 mm; single-side polished) in an oxidation furnace. The wafers were then cleaned with sonication in acetone for 5 min, rinsed with isopropyl alcohol and water for another 2 min, and dried with the flow of nitrogen. A thin film of negative photoresist (AZnLOF 2070, Microchem, Newton, MA) was spin coated (3000 rpm for 30 s) onto the wafer and soft baked at 110 ºC for 6 min. Subsequent UV exposure (280 mJ/cm^2) using a mask aligner (EVG 620, EV Group GmbH, Austria) and development (AZ 726 developer for 3 min) revealed the exposed patterns without photoresist. Metallic layers of Ti (10 nm) and Au (200 nm) were deposited using an electron beam (e-beam) evaporator (Temescal FC-2000) under high vacuum conditions followed by lift-off using ethanol revealed the patterned gold electrodes. The wafers were then diced (ADT 7100 wafer precision dicer) to obtain individual devices. Devices were characterized by SEM analysis using a JEOL (model 6610) instrument operating at an accelerating voltage of 10 kV.

b. Fabrication of Microfluidic Channels. The fabrication of microfluidic channels (Figure S2, Supporting Information) involve a two-step process that include the (i) fabrication of an SU-8 master molds containing three independent microfluidic channels (width, w = 400 μm; height, h = 300 μm; length, l = 25 mm) with 1 mm diameter inlet and outlet ports, and (ii) fabrication of microfluidic channels on PDMS using the master molds. Initially, a layer of negative photoresist (SU-8 2150; MicroChem, MA) was spin coated (1800 rpm) onto a clean silicon wafer (diameter, 100 mm; thickness-1 mm; single-side polished). The wafer was soft baked through a series of step change in temperature (65 °C for 7 min, 95 °C for 60 min, 65 °C for 5 min). Subsequent UV exposure (380 mJ/cm^2) was followed by a post-bake step (from 65 °C for 5 min, 95 °C for 20 min, 65 °C for 3 min). To reveal the fluidic channels the wafers were developed in propylene glycol methyl ether acetate (PGMEA) for 45 min. These

SU-8 masters were then used as molds, on which polydimethylsiloxane (PDMS) prepolymer mixed with its crosslinker (ratio 10:1; Sylgard 184 kit, Dow Corning) was poured, degassed, and allowed to cure in a conventional oven at 65 ºC for 2 h. The cured PDMS replicas were removed from the molds and 1 mm holes were punched into PDMS at either ends of the channel to define the inlet and outlet ports (diameter, 1 mm).

Cell Culture and Isolation of Exosomes. Breast cancer (HER2(+): BT-474; HER2(-): MDA-MB-231) and prostate cancer (PSA(+): PC3) cell lines were maintained in microvesicles depleted serum free Media 171 (Gibco, UK) supplemented with Mammary Epithelial supplement (Gibco, UK), 1% Pencillin/streptomycin and grown in 5% CO_2 at 37 ^{o}C. The conditioned medium from 10^6 cells was collected after 60 h and centrifuged at 2000 × g for 30 min to eliminate cell contamination (*e.g.*, cells and debris). Exosomes were isolated using Total Exosome isolation reagent (Life Technologies) as per manufacturer's instructions. Briefly, the supernatant was transferred to a new tube and the isolation reagent was added to the tube in the ratio 2:1. The samples were incubated overnight at 4 ^{o}C followed by filtration using 0.22 µm filter and centrifugation at 10000 × g for 1 h to obtain exosome pellets. Exosome pellets were then resuspended in 100 µL PBS (10 mM, pH 7.0) and stored at -20 ^{o}C for further use.

Cryo-Transmission Electron Microscopy (Cryo-TEM). For cryo-TEM, 4 µL of exosome preparations were directly adsorbed onto lacey carbon grids (Quantifoil, Germany) and plunged into liquid ethane, using an FEI Vitrobot Mark 3 (FEI Company, The Netherlands). Grids were blotted at 100% humidity at 4 ºC for about 3-4 s. Frozen/vitrified samples were imaged using Tecnai T12 Transmission Electron Microscope (FEI Company) operating at an acceleration voltage of 120 kV. Images were taken at 30,000x magnification, (approximate

dose of 13.6 electrons/Å^2), using an FEI Eagle 4k CCD (FEI Company), and SerialEM image acquisition software.

Dynamic Light Scattering Analysis. Exosome samples were prepared by spiking 1 μL of isolated exosomes in PBS (10 mM, pH 7.0) to obtain the desired dilution (1:1000). The size and zeta potentials of the nanovesicles were measured using a dynamic laser scattering (DLS) instrument (Zetasizer 3000HSA, Malvern Instrument) at 25 ^{o}C under a refractive index of 1.33 and viscosity of 0.89 mPa.s .

Device functionalization. Prior to functionalization, the electrodes were cleaned by sonication in acetone for 5 min, rinsed with isopropyl alcohol and water for another 2 min, and dried with the flow of nitrogen. The array of gold microelectrode pairs within the capture domain of the channel were then modified with the capture antibody (*e.g.*, anti-HER2, anti-CD9 and/or anti-PSA) using avidin-biotin chemistry (Figure 2) in a three step process. Initially, devices were incubated in biotinylated BSA (200 μg/mL in PBS, Invitrogen) solution for 2 h followed by coupling with streptavidin (100 μg/mL in PBS, Invitrogen) for 1 h at 37 ^{o}C. Streptavidin conjugated channels were then coated with biotinylated capture antibody (*e.g.*, anti-HER2 and/or anti-PSA or anti-CD9; 10 μg/mL in PBS, R&D systems) for another 2 h. Channel was flushed three times with PBS (10 mM, pH 7.0) to remove any unbound molecules after each step. Each of the surface modification steps (*e.g.*, biotinylated BSA, streptavidin, and capture antibody) was performed manually by filling the microchannel with corresponding solution to specifically modify the array of gold electrodes within the capture domain. PDMS containing the microchannels was then aligned manually onto the electrodes and sandwiched between custom built device holders (Figure S3,

Supporting Information) for samples to be filled and withdrawn via inlet and outlet ports, respectively.

Exosome capture and detection. The concentration of exosomes in the isolated pellets was obtained using qNano measurements performed as described previously.[18] Exosome samples were prepared by spiking 1 µL of isolated exosomes in PBS (10 mM, pH 7.0) to obtain the desired dilution (1:1000). Concentration measurements were obtained by calibrating particle count rate recordings against a reference particle suspension (polystyrene beads, d = 115 nm). Samples were then prepared by spiking designated volumes of isolated exosomes in PBS (1 mM, pH 7.0) to obtain the desired sample dilutions (1:200 to 1:3000) in a given volume (500 µL). Serum samples (1 mL) of two breast cancer patients were obtained from Ventyx Wesley Research Institute Tissue Bank, Brisbane, Australia and stored in -80 ^{o}C until further use. Immunohistochemical expression analysis suggested overexpression (3+: Patient A) and very low expression (1+; Patient B) of HER2 in these patient samples. The small and large electrodes within the long channel of the ac-EHD devices (Figure S1,S3, Supporting Information) were connected to a signal generator (Agilent 33220A Function Generator, Agilent Technologies, Inc., CA) *via* gold connecting pads. Samples were then placed in the inlet reservoirs of the devices and driven through the channel by applying ac-EHD field. The field strength was applied for 30 min with 15 min intervals (without fluid flow) for a total pumping time of approximately 2 h. Control experiments were performed in the absence of ac-EHD field under pressure driven flow conditions using a syringe pump (PHD 2000, Harvard apparatus). Detection antibody FITC conjugated anti-HER2 (2 µg/mL; Invitrogen, UK) was driven through the channels under ac-EHD and/or pressure driven flow conditions. For anti-PSA and/or anti-CD9 functionalized devices, the detection antibody HRP conjugated anti-PSA (2 µg/mL; abcam) and/or FITC conjugated anti-CD9 (2 µg/mL; abcam) was driven

through the channels under ac-EHD fluid flow. anti-HER2 functionalized devices were imaged under a fluorescence microscope (Nikon eclipse Ni-U upright microscope) to obtain fluorescence images of the captured exosomes. anti-HER2 and/or anti-CD9 functionalized devices were then further incubated with anti-fluorescein HRP (1:1000; abcam) antibody for 45 min. Channels were flushed three times with PBS (1 mM, pH 7.0) after subsequent steps to remove any unbound molecules. 80 µL of 3,3',5,5'-tetramethylbenzidine (TMB) solution was driven though the channels manually and the colorimetric reaction was allowed to proceed for 5 min to facilitate naked eye detection from the resulting colour change in solution. The colorimetric solution was withdrawn manually from the device using a micropipette and collected in an eppendorf for subsequent absorbance measurements. Absorbance measurements were obtained using a UV-Visible spectrophotometer (Shimadzu UV-2450, Shimadzu Corp.) and absorbance data was acquired using UVProbe (Ver. 2.3.1) data acquisition software.

RESULTS AND DISCUSSION

To investigate the applicability of *nanoshearing* phenomenon, we constructed a multiplexed microfluidic device (see Experimental for design and fabrication details; Figure 3a,b and Figure S1,S2, Supporting Information) with three independent microchannels comprehending a long array of consecutively placed asymmetric electrode pairs within each channel. The device was sandwiched between custom built holders with the small and large electrodes within the long channel being connected to a signal generator (see Figure S3, Supporting Information for experimental setup). The application of an alternating potential difference to each pair of asymmetric electrodes results in a nonuniform electric field $\boldsymbol{E}$ (Figure 1) that induces charges in the double layer (λ_D = Debye length). The lateral variation in the total amount of induced double layer charges and spatial distribution of charges on the

electrode surface give rise to stronger lateral forces on the large electrode, resulting in fluid flow towards the large electrode.[10,16] This lateral flow due to surface shear forces generated within nanometers (λ_D = ~ 4 nm, calculated for 1 mM phosphate buffer saline (PBS) using Debye-Huckel approximation[19] and use of the equation described in ref.11) of an electrode surface is unidirectional. This unidirectional flow causes analytes in solution to be dragged by the flow, and their interaction with the surface is significantly enhanced (Figure 1).

To demonstrate the utility of *nanoshearing* effect for exosome detection, we tested the capture and detection of exosomes obtained from breast cancer cell lines expressing human epidermal growth factor receptor 2 (HER2), an important breast cancer therapeutic target.[20] Exosomes were isolated (see Experimental for exosome isolation) from breast cancer cell line BT-474 showing HER2 overexpression.[21] Western blotting analysis verified the HER2 expression in these BT-474 derived exosomes (data not shown). Characterization of the isolated exosomes using cryo-Transmission Electron Microscopy (TEM) suggested that predominantly these vesicles contained double-walled lipid membrane layers (Figure 3c). Dynamic Light Scattering (DLS) measurements (Figure 3d) suggested that the large population of exosomes (*e.g.*, 98±0.7%) falling within the size range of 30-350 nm with the average vesicle size determined to be 111±3.07 nm. The morphological and physical characteristics determined using these techniques corroborate with previous evidences[22,23] suggesting that these nanovesicles are probably of exosomal origin and were used for further capture experiments using multiplexed ac-EHD devices.

The critical determinants that comprehend the tuning capability of surface shear forces and concomitant micromixing include the ac frequency and amplitude. To determine the optimal ac-EHD induced forces for exosome capture, the electrode surface on individual channels of the device was initially functionalized (see Experimental and Figure 2 for exosome capture and detection) with anti-HER2 capture antibody. Samples containing

isolated exosomes (1:200 in PBS; see Experimental for sample preparation) were driven through the devices under the frequency (*f*) range of 600 Hz-100 kHz at constant amplitude (V_{pp}) of 100 mV. The captured exosomes were detected via a rapid (~5 min) on-chip naked eye read-out obtained due to the oxidation of TMB. The colorimetric solution was collected manually from the device and the corresponding absorbance measurements using UV-visible spectroscopy measurements (maximum absorbance at 652 nm; A_{652nm}) provided quantitative information on the captured exosomes. Figure 4a,b demonstrates spiked exosome samples under the frequency range of 600 Hz -100 kHz at V_{pp} = 100 mV. Capture performance of the device was found to be a function of the applied frequency as observed from the initial sharp colour change to deep blue (600 Hz and1 kHz in Figure 4a) and a gradual change in colour to a clear solution (1 kHz- 100 kHz in Figure 4a) with increase in frequency. UV-Visible spectroscopy measurements (Figure 4b, inset) and absorbance peak at 652 nm (A_{652nm}; Figure 4b) also demonstrated a similar trend in capture levels thereby further verifying these observations. The resulting higher level of capture at low field (*e.g.*, f = 1 kHz and V_{pp} = 100 mV) is probably due to the effective stimulation of the fluid flow around the capture domain that can maximize the effective exosome-antibody collisions (a condition where shear force < antibody-exosome binding force). In contrast, at higher frequencies the ac-EHD forces (*e.g.*, f = 100 kHz, V_{pp} = 100 mV) result in stronger fluid flow which could ablate exosome recognition (a condition where shear forces > antibody-antigen affinity interaction) and decrease the capture level. Therefore, the ac-EHD force resulted from the frequency of 1 kHz and amplitude of 100 mV was used for further studies in demonstrating the application of ac-EHD induced *nanoshearing* phenomenon in detecting exosomes.

To validate the specificity and accuracy of exosome capture and detection, control experiments were performed under applied ac-EHD field strength of f = 1 kHz and V_{pp}= 100 mV using samples spiked with (1:200 in PBS) and without exosomes. In the case of samples

without exosomes, negligible nonspecific binding of the FITC conjugated detection antibody was observed under ac-EHD field as evident from the absorption spectra (red; Figure S4a, Supporting Information). Representative fluorescence images (see Experimental for details) of the detected exosomes and nonspecifically bound detection antibody are shown in Figure S4b,c, Supporting Information. To further investigate the specificity of detection, we performed additional control experiments using (i) devices functionalized without anti-HER2 capture antibody and (ii) devices without FITC conjugated anti-HER2 detection antibody. Samples containing spiked exosomes (1:200 in PBS) were driven through the devices under the applied ac-EHD flow conditions (f = 1 kHz and V_{pp}= 100 mV). As can be seen in Figure S5a,b, Supporting Information, devices without capture (blue; Figure S5a, Supporting Information) and/or detection antibody (green; Figure S5b, Supporting Information) did not have a substantial effect in altering detection capabilities of the devices owing to negligible nonspecific binding of the detection antibody (*e.g.*, device without capture antibody) and the absence of HRP for TMB oxidation (*e.g.*, device without detection antibody) respectively. This data suggests that ac-EHD induced *nanoshearing* can facilitate specific capture of target exosomes by minimising background response from detection antibody.

Tetraspanin superfamily proteins (*e.g.*, CD9, CD63, CD81, CD82 etc.) are one of the most abundant protein markers found in exosomes isolated from virtually any cell type.[1] To investigate the selectivity of capture and detection, we performed capture experiments on anti-CD9 functionalized devices using exosomes isolated from HER2(+) BT-474 and HER2(-) MDA-MB-231 breast cancer cell lines. Figure S5c, Supporting Information, demonstrates capture performance of the device for spiked samples containing exosomes (1:200 in PBS) isolated from BT-474 and MDA-MB-231 cell lines. Under the applied field strength (f = 1 kHz and V_{pp}= 100 mV), the capture performance was found to be almost similar for exosome samples isolated from both BT-474 (black, Figure S5c, Supporting

Information) and MDA-MB-231 (red; Figure S5c, Supporting Information) cell lines. These results support the fact that our approach is highly selective considering the specific capture of exosomes derived from HER2(+) and HER2(-) cell lines using anti-CD9 functionalized devices. To further verify the selectivity and specificity of our approach, we then performed an additional capture experiments on anti-HER2 functionalized devices using exosomes isolated from HER2(-) MDA-MB-231cell lines and observed a negligible capture levels (blue; Figure S5c, Supporting Information). This is possibly due to the lack of HER2 expression in MDA-MB-231cell lines and cell derived exosomes. This data indicates that our approach is selective in capturing exosomes of interest in spiked samples, rather than any associated microvesicles, cell debris or protein molecules that could have possibly been isolated during the exosome extraction procedure.

To assess the dynamic range and lower limit of detection (LOD) of our device, designated volumes of exosomes were spiked in PBS to obtain desired dilutions (1:200 to 1:3000) and run on anti-HER2-functionalized devices under the optimal ac field strength of f = 1 kHz and V_{pp} = 100 mV. The approximate concentration of exosomes in these samples was calculated from qNano measurements (see Experimental for details) and was found to range from 4.15×10^4 – 2.76×10^3 exosomes/µL. Under the applied ac-EHD field, colorimetric readouts (Figure 5a) and corresponding absorbance data (Figure 5b) indicate that the device was sensitive enough to detect samples containing approximately >2760 exosomes/µL (*i.e.*, 1:3000 in PBS). The linear dynamic range of detection was found to be 2.76×10^3 (1:3000 in PBS) to 4.15×10^4 exosomes/µL (*i.e.*, 1:200 in PBS) with the lower limit of detection (LOD) approximately >2760 exosomes/µL. The average number of exosomes obtained from biological fluids (*e.g.*, plasma, cell culture media, serum, urine etc.) range from 8.0×10^3 to 5.0×10^5 exosomes/µL.[23,24] Thus, this level of detection (>2760 exosomes/µL) indicate that our method could potentially be suitable for analysing exosomes.

However, we believe further optimization to the protocol and device geometry (*e.g.*, length, width, and height of the channel; spacing between electrodes in the long array of asymmetric pairs) could further improve the capture performance of our device to meet clinically useful detection limits.

We then compared the capture performance under the optimal ac-EHD flow to that of a hydrodynamic flow using a pressure-driven system (*via* a syringe pump) to drive fluid through the devices with the similar flow rate (7 $\mu Lmin^{-1}$; an equivalent to the flow generated under the optimal ac-EHD field of f = 1 kHz and V_{pp}= 100mV). Samples containing two different concentrations of exosomes (1:200 and 1:1000 in PBS) were driven through the devices under ac-EHD and pressure driven flow conditions. Figure S6a,b, Supporting Information, shows the capture performance of the device under ac-EHD induced fluid flow and pressure driven flow conditions. For both concentrations, colorimetric detection and corresponding absorbance data yielded a 5-fold increase in capture level and a 3-fold enhancement in detection sensitivity (LOD = 2750 exosomes/μL for ac-EHD *vs* LOD = 8300 exosomes/μL for hydrodynamic flow; (n = 3)) under ac-EHD in comparison with pressure driven flow based controls. The enhanced exosome capture with the use of ac-EHD induced fluid flow compared to the pressure driven flow based devices may be attributed to the synergistic effect of the geometric arrangements of the antibody-functionalized microelectrode pairs within the channel, ac-EHD induced *nanoshearing* and concomitant fluid mixing phenomena.

To demonstrate the multiplexing capability of our device and also further examine the effect of *nanoshearing* to capture low concentration of target exosomes in large excess of non-target exosomes, microvesicles and cellular proteins, individual channels of the device was functionalized (Figure 6a) with anti-HER2 (*e.g.*, channel-1) and anti-PSA (*e.g.*, channel-2) capture antibody. Target exosomes derived from a specific cell line (HER2(+) and/or

PSA(+)) were spiked with large excess of non-target exosomes derived from two nonspecific cell lines. For channel 1, specific exosomes (1:3000 in PBS) derived from BT-474 were spiked with two nonspecific exosomes (for both cases, 1:200 in PBS) from MDA-MB-231 and PC3 cell lines. For channel 2, exosomes (1:3000) derived from PC3 cell line were used as target exosomes while exosomes (1:200) from MDA-MB-231 and BT-474 cell lines were used as nonspecific targets. Figure 6a demonstrates duplex detection of spiked cell derived exosome samples under the applied ac field strength of f = 1 kHz and V_{pp} = 100 mV. It was clearly evident that the capture and detection performance of the device was highly reproducible with the device being sensitive enough to detect low concentration (1:3000) of target BT-474 (blue; channel-1, Figure 6a) and PC3 (green; channel-2, Figure 6a) derived exosomes in the presence of non-target exosomes (15 fold higher concentration than target exosomes). We also validated the specificity of capture by performing additional control experiments on anti-HER2 functionalized devices using (i) samples spiked only with non-target exosomes derived from MDA-MB-231 and PC3 cell lines (*i.e.*, without target BT-474 derived exosomes) in PBS (for both cases, 1:200) and (ii) only PBS buffer (*i.e.*, without target and non-target exosomes). Under the applied field strength of f = 1 kHz at V_{pp} = 100 mV, a very low background response from the detection antibody (black; Figure S7, Supporting Information) and/or nonspecific exosomes (red; Figure S7, Supporting Information) was observed that further verified the high specificity of immunocapture. This level of background response suggests that our method is applicable to detect exosomes at >1:3000 concentration in the presence of 15-fold excess of nonspecific exosomes in the heterogeneous samples. Thus, *nanoshearing* can be an effective tool for the enhancement of target capture even at low concentrations and is comparable to the existing methodologies for avoiding nonspecific adsorption using molecular coatings[25] and zwitterion complexes.[26] Furthermore, this detection limit and device performance is comparable with recent

microfluidic technologies for capture and detection of extracellular vesicles from complex biological samples based on immunoaffinity capture,[7] silicon nanowires traps on micropillars,[8] and nanoporous membranes[9] that rely on size based exclusion and exosomal marker based immunocapture. Additionally, the key to the functionality and simplicity of our approach includes: (i) stimulation of fluid flow around the antibody-modified electrodes (*i.e.* fluid *nanoshearing* in the electrode/solution interface) improve the analysis performance of exosome targets *via* enhancing the number of sensor-target collisions as well as physically displacing nonspecifically adsorbed species from the electrode surface, (ii) use of a multiplexed device enables the analysis of multiple exosome targets isolated from complex biological fluids (*e.g.*, cell culture media, serum), and (iii) on-chip naked eye detection coupled with absorbance measurements provides a rapid quantification tool potentially suited for clinical analysis of these nanovesicles.

Finally, to investigate the diagnostic potential of our method, we performed experiments using HER2(+) (Patient A) and HER2(-) (Patient B) breast cancer patient serum (see Experimental for sample details). Individual channels of the devices were functionalized with anti-HER2 capture antibody and samples (500 μL for each channel) were driven through the devices (Patient A: channel-1; Patient B: channel-2) under optimal ac-EHD field strength (f = 1 kHz and V_{pp} = 100 mV). Colorimetric readouts (Figure 6b) suggested high capture levels in the HER2(+) Patient A sample whilst negligible capture levels were observed in HER2(-) Patient B serum. The corresponding absorbance measurements (Figure 6b) corroborate with these observations. The maximum absorbance (A_{652nm}) data suggested that the approximate concentration of exosomes in these samples were 2×10^4 (Patient A) and 3.7×10^3 exosomes/μL (Patient B), respectively. Furthermore, to verify the selectivity and specificity of capture, these patient serum samples (500 μL) were driven through anti-CD9 functionalized devices (Patient A: channel-1; Patient B: channel-2) under the optimal ac-

EHD field strength (f = 1 kHz and V_{pp} = 100 mV). In this case, the capture performance of the device was found to be almost similar (Figure 6c) for both patient (HER2(+) and HER2(-)) serum samples. The results obtained from anti-HER2 and anti-CD9 functionalized devices support the fact that our approach is selective and specific in isolating exosomes rather than any nonspecific microvesicles, cell debris or protein molecules present in the patient samples. These data indicate that our approach is potentially suitable for the isolation of exosomes from clinical samples and can find its relevance as a simple diagnostic tool in clinical settings.

CONCLUSIONS

We have developed a novel microfluidic platform technology for rapid, multiplexed and highly specific on-chip detection and quantification of exosomes using the unique capacity of ac-EHD induced *nanoshearing*. The versatility of our approach lies in (i) the use of asymmetric microelectrode pairs as fluid pumps (avoids use of additional pumps, valves, etc) and capture/detection domain during simultaneous capture of multiple target exosomes under ac-EHD induced fluid flow and (ii) the potential to be applicable for essentially any biochemical assay based on immunocapture (via modifying the device with any antibody specific to any disease biomarker). We demonstrate the ability of this approach to enhance the detection capabilities of the device (*e.g.*, approximately > 2750 exosomes/μL and 5 fold increase in capture and detection performance in comparison to hydrodynamic fluid flow) and also specifically isolate exosomes from breast cancer patient samples. We envisage that this proof-of-concept study offering a *tunable* control of the target capture process and enabling the detection of multiple exosome targets can potentially establish its significance as a rapid exosome quantification tool that can find promising applications in cancer diagnostics.

AUTHOR INFORMATION

Corresponding Authors

*Email: m.shiddiky@uq.edu.au (MJAS); m.trau@uq.edu.au (MT)

Tel: +61-7-33464178; Fax: +61-7-33463973

Notes

The authors decleare no competing financial interest.

ACKNOWLEDGEMENTS

This work was supported by the ARC DECRA (DE120102503) and ARC DP (DP140104006). We acknowledge funding from the National Breast Cancer Foundation of Australia via National Collaborative Research Grants (CG-12-07). We also acknowledge Mr. Will Anderson and Ms. Rebecca Lane for performing the DLS and qNano measurements. The fabrication work was performed at Queensland node of the Australian National Fabrication Facility (Q-ANFF) and microscopy analysis was performed at the Australian Microscopy and Microanalysis Research Facility (AMMRF).

ASSOCIATED CONTENT

SUPPORTING INFORMATION

Design, fabrication, and additional data. This material is available free of charge via the Internet at http://pubs.acs.org.

REFERENCES

(1) Théry, C.; Zitvogel, L.; Amigorena, S. *Nat. Rev. Immunol.* **2002**, *2*, 569.

(2) Booth, A. M.; Fang, Y.; Fallon, J. K.; Yang, J. M.; Hildreth, J. E.; Gould, S. J. *J. Cell Biol.* **2006**, *172*, 923-35.

(3) Skog, J.; Würdinger, T.; van Rijn, S.; Meijer, D. H.; Gainche, L.; Sena-Esteves, M.; Curry, Jr., W. T.; Carter, B. S.; Krichevsky, A. M.; Breakefield, X. O. *Nat. Cell. Biol.* **2008**, *12*, 1470-76.

(4) Valadi, H.; Ekström, K.; Bossios, A.; Sjöstrand, M.; Lee, J. J.; Lötvall, J. O. *Nat. Cell Biol.* **2007**, *9*, 654-59.

(5) Cantin, R.; Diou, J.; Bélanger, D.; Tremblay, A. M.; Gilbert, C. *J. Immunol. Methods*, **2008**, *338*, 21–30.

(6) Théry, C.; Clayton, A.; Amigorena, S.; Raposo, G. *Current Protocols in Cell Biology*, ed. K. Morgan, John Wiley, New York, **2006**, p. UNIT *3.22*.

(7) Chen, C.; Skog, J.; Hsu, C.-H.; Lessard, R. T.; Balaj, L.; Wurdinger, T.; Carter, B.S.; Breakefield, X. O.; Toner, M.; Irimia, D. *Lab Chip* **2010**, *10*, 505-511.

(8) Davies, R. T.; Kim, J.; Jang, S. C.; Choi, E.-J.; Gho, Y. S.; Park, J. *Lab Chip* **2012**, *12*, 5202-5210.

(9) Wang, Z.; Wu, H.-J.; Fine, D.; Schmulen, J.; Hu, Y.; Godin, B.; Zhang, J. X. J.; Liu, X.; *Lab Chip* **2013**, *13*, 2879-2882.

(10) Vaidyanathan, R.; Shiddiky, M. J. A.; Rauf, S.; Dray, E.; Tay, Z.; Trau, M. *Anal. Chem.* **2014**, *86*, 2042-49.

(11) Shiddiky, M. J. A.; Vaidyanathan, R.; Rauf, S.; Tay, Z.; Trau, M. *Sci. Rep.* **2014**, *4*, 3716.

(12) Vaidyanathan, R.; Rauf, S.; Dray, E.; Shiddiky, M. J. A.; Trau, M. *Chem. Eur. J.* **2014**, *20*, 3721-29.

(13) Vaidyanathan, R.; Rauf, S.; Shiddiky, M. J. A.; Trau, M. *Biosens. Bioelectron.* **2014**, *61*, 184-91.

(14) Rauf, S.; Shiddiky, M. J. A.; Trau, M. *Chem. Commun.* **2014**, *50*, 4813-15.

(15) Marquez, L. A.; Dunford, H. B. *Biochemistry*, **1997**, *36*, 9349-55.

(16) Brown, A. B. D.; Smith, C. G.; Rennie, A. R.; *Phys. Rev. E.* **2001**, *63*, 016305.

(17) Ramos, A.; González, A.; Castellanos, A.; Green, N. G.; Morgan, H., *Phys.Rev. E.* **2003**, *67*, 056302.

(18) Seth Roberts, G.; Yu, S.; Zeng, Q.; Chan, L. C. L.; Anderson, W.; Colby, A. H.; Grinstaff, M. W.; Reid, S.; Vogel, R. *Biosens. Bioelectron.* **2014**, *31*, 17-25.

(19) Hunter, R. J.; *Foundations of colloidal science*, Oxford University Press Inc., New York, **1987**.

(20) Carlsson, H.; Nordgren, H.; Sjöström, J.; Wester, K.; Villman, K.; Begtsson, N. O.; Ostenstad, B. Lundqvsit, H.; Blomqvist, C., *Br J Cancer* **2004**, *90*, 2344-2348.

(21) Subik, K.; Lee, J. F.; Baxter, L.; Strzepek, T.; Costello, D.; Crowley, P.; Xing, L.; Hung, M. C.; Bonfiglio, T.; Hicks, D. G.; Tang, P., *Breast Cancer* **2010**, *4*, 35-41.

(22) Coleman, B. M.; Hanssen, E.; Lawson, V. A.; Hill, A. F. *FASEB J.* **2012**, *26*, 4160-73.

(23) de Vrij, J.; Maas, S. L.; van Nispen, M.; Sena-Esteves, M.; Limpens, R. W.; Koster, A. J.; Leenstra, S.; Lamfers, M. L.; Broekman, M. L. *Nanomedicine (Lond).* **2013**, *8*, 1443-58.

(24) Huang, X.; Yuan, T.; Tschannen, M.; Sun, Z.; Jacob, H.; Du, M.; Liang, M.; Dittmar, R. L.; Liu, Y.; Liang, M.; Kohli, M.; Thibodeau, S. N.; Boardman, L.; Wang, L. *BMC Genomics.* **2013,** *14*, 319.

(25) Ostuni, E,; Chen, C. S.; Ingber, D. E.; Whitesides, G. M. *Langmuir* **2001**, *17*, 2828-2834.

(26) Banerjee, I.; Pangule, R. C.; Kane, R. S. *Adv. Mat.* **2011**, *23***,** 690-718.

FIGURE CAPTIONS

Figure 1. Schematic representation of ac-EHD induced tunable *nanoshearing* for the specific capture of exosomes (appeared as white spherical particles). The large and small electrodes in an asymmetric electrode pair form the cathode and anode (or *vice versa*) of an electrolytic cell. The application of an ac field ***E*** across the electrode pairs results in nonuniform forces on the large and small electrodes due to the lateral variation in number of induced charges and their spatial distribution with the resultant force giving rise to unidirectional movement towards the larger electrode. These shear forces generated within nanometers (λ_D) of an electrode surface engender fluid flow vortices and induce fluid mixing that can displace weakly bound nonspecific species and hence termed as *nanoshearing*.

Figure 2. Schematic representation of device functionalization, exosome capture and colorimetric detection of captured exosomes.

Figure 3. (a) Schematic of a multiplexed microfluidic device for exosome detection comprising of three independent channels. (b) Corresponding scanning electron microscopy (SEM) image of the enlarged segment of the device. (C) Cryo-TEM images of BT-474 cell derived exosomes demonstrating size and vesicular compartments such as membrane layers. (D) Dynamic light scattering measurements of BT-474 cell derived exosomes demonstrating the size range of the vesicles based on their scattered light intensity.

Figure 4. (a) Colorimetric detection of BT-474 cell derived exosomes spiked in 500 µL PBS (1:200) under the frequency range f = 600 Hz- 100 kHz at V_{pp} = 100 mV. (b) Absorbance peak at 652 nm (A_{652nm}) for exosomes spiked in PBS (1:200) under the frequency range f = 600 Hz- 100 kHz at V_{pp} = 100 mV. Each data point represents the average of three separate

trials *(n = 3)* and error bars represent standard error of measurements within each experiment. Inset shows corresponding UV-Vis absorption spectra obtained from respective colorimetric solutions.

Figure 5. (a) Colorimetric detection of samples containing spiked BT-474 cell derived exosomes in PBS at desired dilutions (1:200 to 1:3000) under ac-EHD field strength of f = 1 kHz at V_{pp} = 100 mV. (b) Absorbance peak at 652 nm (A_{652nm}) for the detected BT-474 cell derived exosomes from spiked PBS samples at desired dilutions (1:200 to 1:3000) under ac-EHD field strength of f = 1 kHz at V_{pp} = 100 mV. Each data point represents the average of three separate trials *(n = 3)* and error bars represent standard error of measurements within each experiment. Inset shows corresponding UV-Vis absorption spectra obtained from respective colorimetric solutions.

Figure 6. (a) UV-Vis absorption spectra of samples spiked with nonspecific exosomes derived from MDA-MB-231 (1:200) and PC3 or BT-474 (1:200) cell lines in PBS along with target HER2(+) BT-474 (blue; channel-1) or PSA(+) PC3 (green; channel-2) derived exosomes (1:3000) under the ac-EHD field strength of f = 1 kHz at V_{pp} = 100 mV. Inset shows naked eye detection of the captured BT-474 (channel-1) and PC3 (channel-2) derived exosomes under the applied ac-EHD field strength. (b,c) UV-Vis absorption spectra of HER2(+) (Patient A; red) and HER2(-) (Patient B; blue) breast cancer patient serum driven through (b) anti-HER2 and (c) anti-CD9 functionalized devices under the ac-EHD field strength of f = 1 kHz at V_{pp} = 100 mV. Inset shows naked eye detection of the captured exosomes.

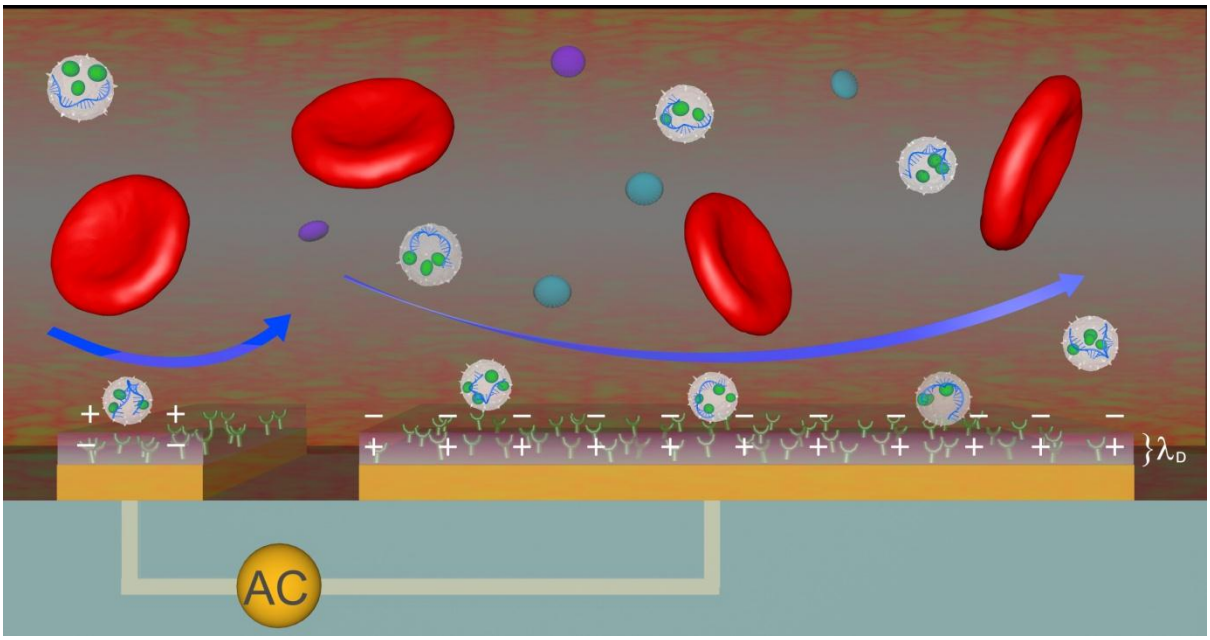

Figure 1.

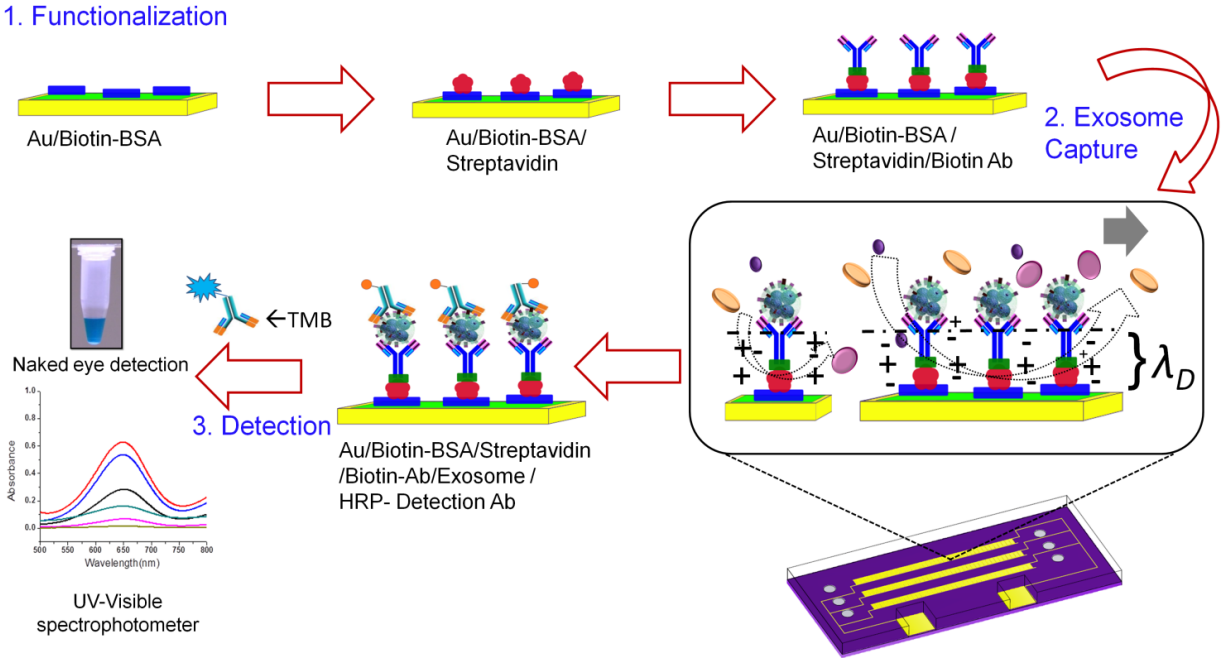
1. Functionalization
Au/Biotin-BSA
Au/Biotin-BSA/
Streptavidin
Au/Biotin-BSA /
Streptavidin/Biotin Ab
2. Exosome
Capture
λ_D
Au/Biotin-BSA/Streptavidin
/Biotin-Ab/Exosome /
HRP- Detection Ab
3. Detection
←TMB
Naked eye detection
Absorbance
Wavelength(nm)
UV-Visible
spectrophotometer

Figure 2.

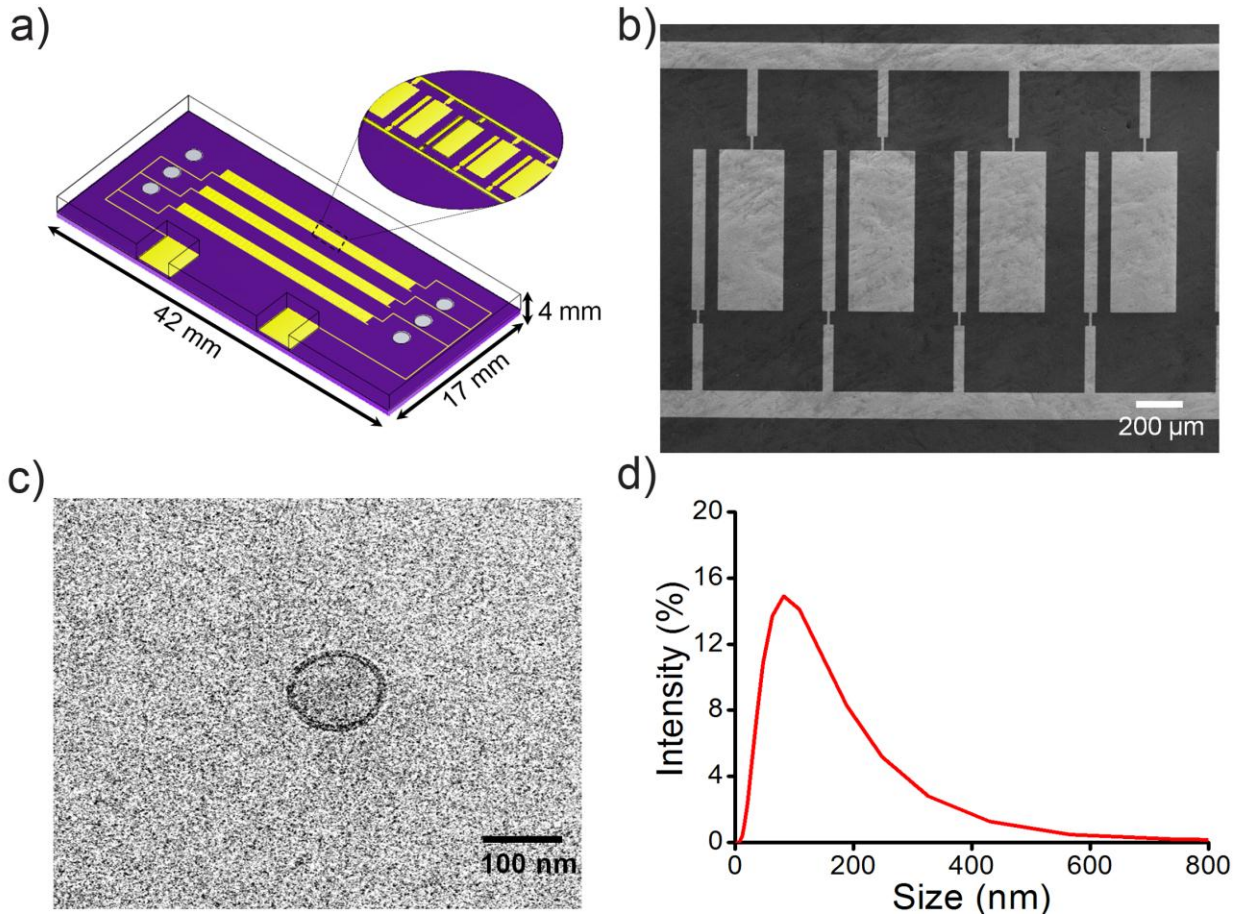
a)
42 mm
17 mm
4 mm
b)
200 µm
c)
100 nm
d)
Intensity (%)
Size (nm)
0
4
8
12
16
20
0
200
400
600
800

Figure 3.

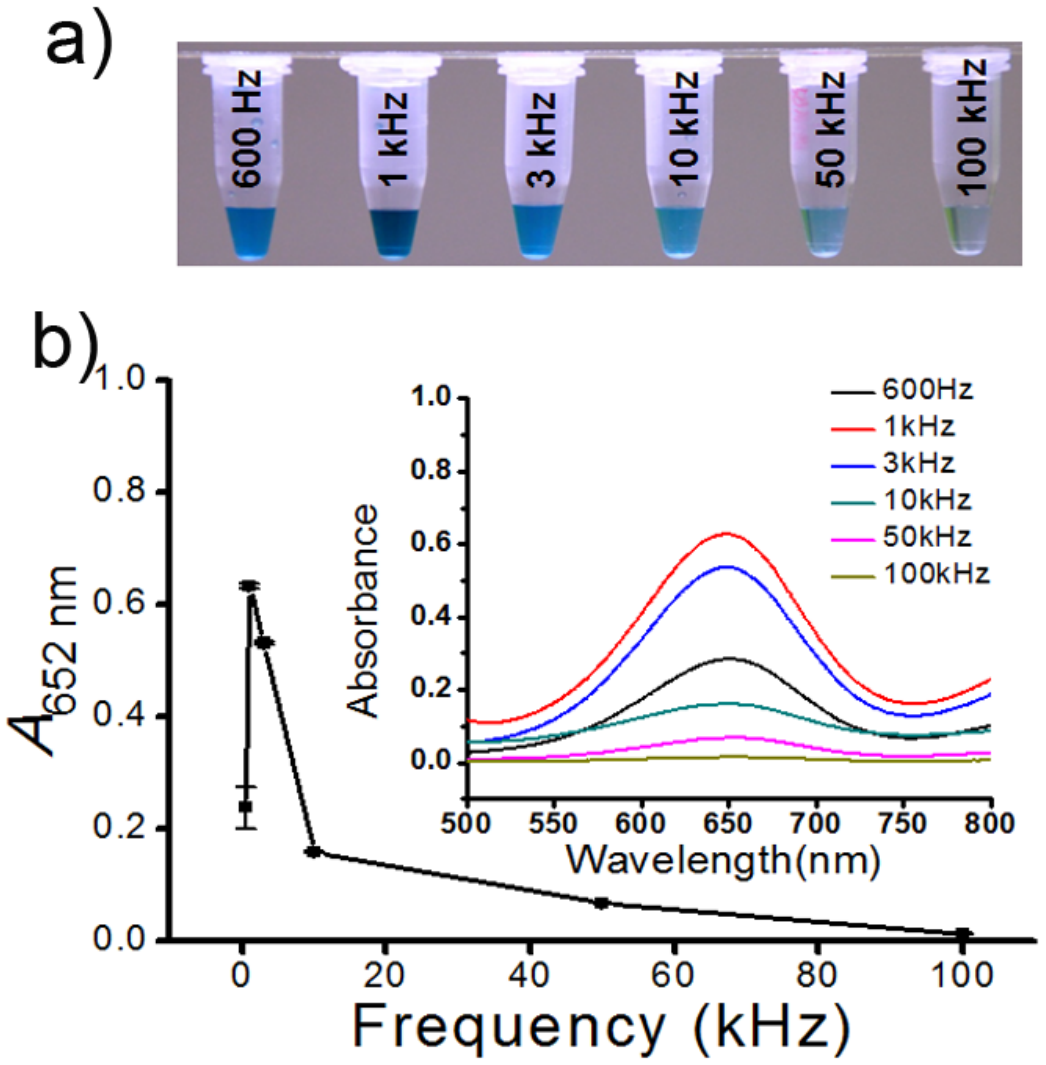
a)
600 Hz
1 kHz
3 kHz
10 kHz
50 kHz
100 kHz
b)
$A_{652\ nm}$
Frequency (kHz)
Absorbance
Wavelength(nm)
600Hz
1kHz
3kHz
10kHz
50kHz
100kHz

Figure 4.

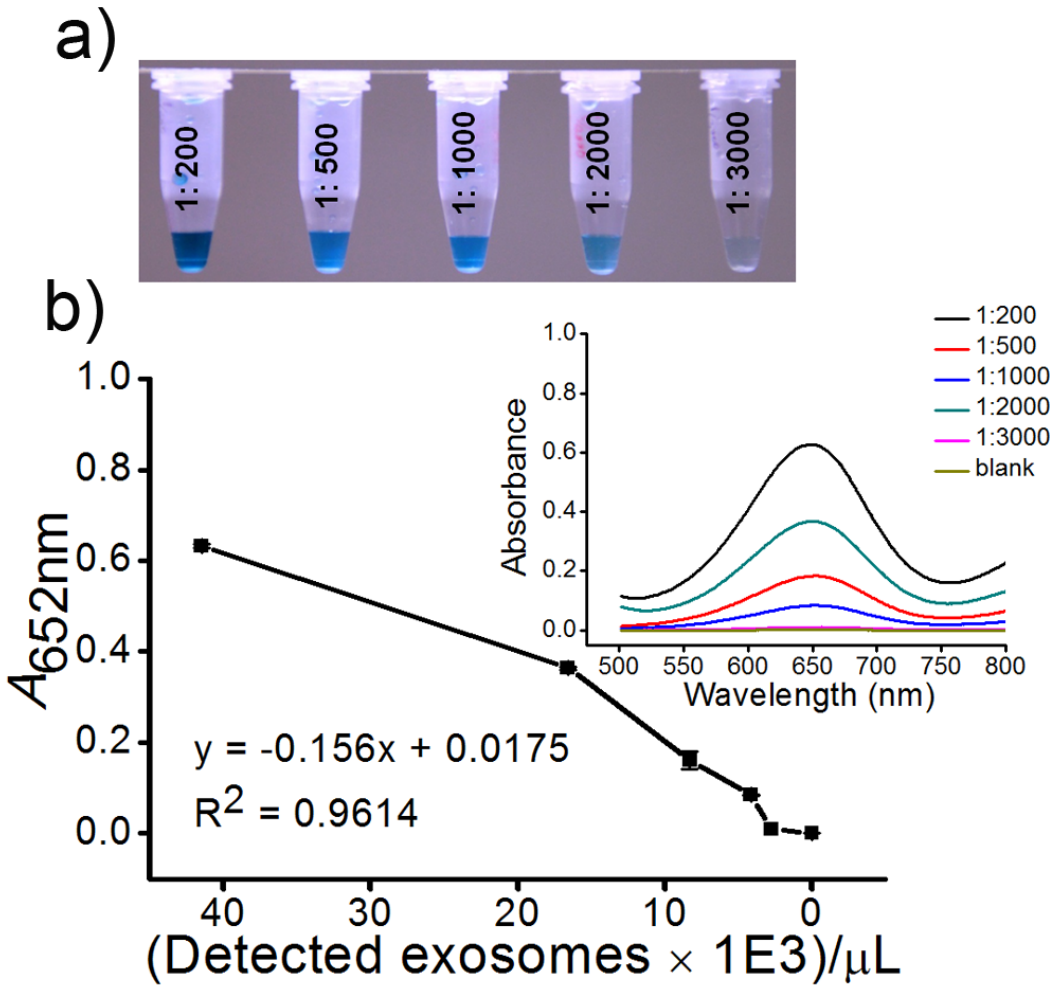
a)
1: 200
1: 500
1: 1000
1: 2000
1: 3000
b)
1.0
0.8
0.6
0.4
0.2
0.0
A652nm
y = -0.156x + 0.0175
R2 = 0.9614
40
30
20
10
0
(Detected exosomes × 1E3)/μL
Absorbance
1.0
0.8
0.6
0.4
0.2
0.0
500
550
600
650
700
750
800
Wavelength (nm)
1:200
1:500
1:1000
1:2000
1:3000
blank

Figure 5.

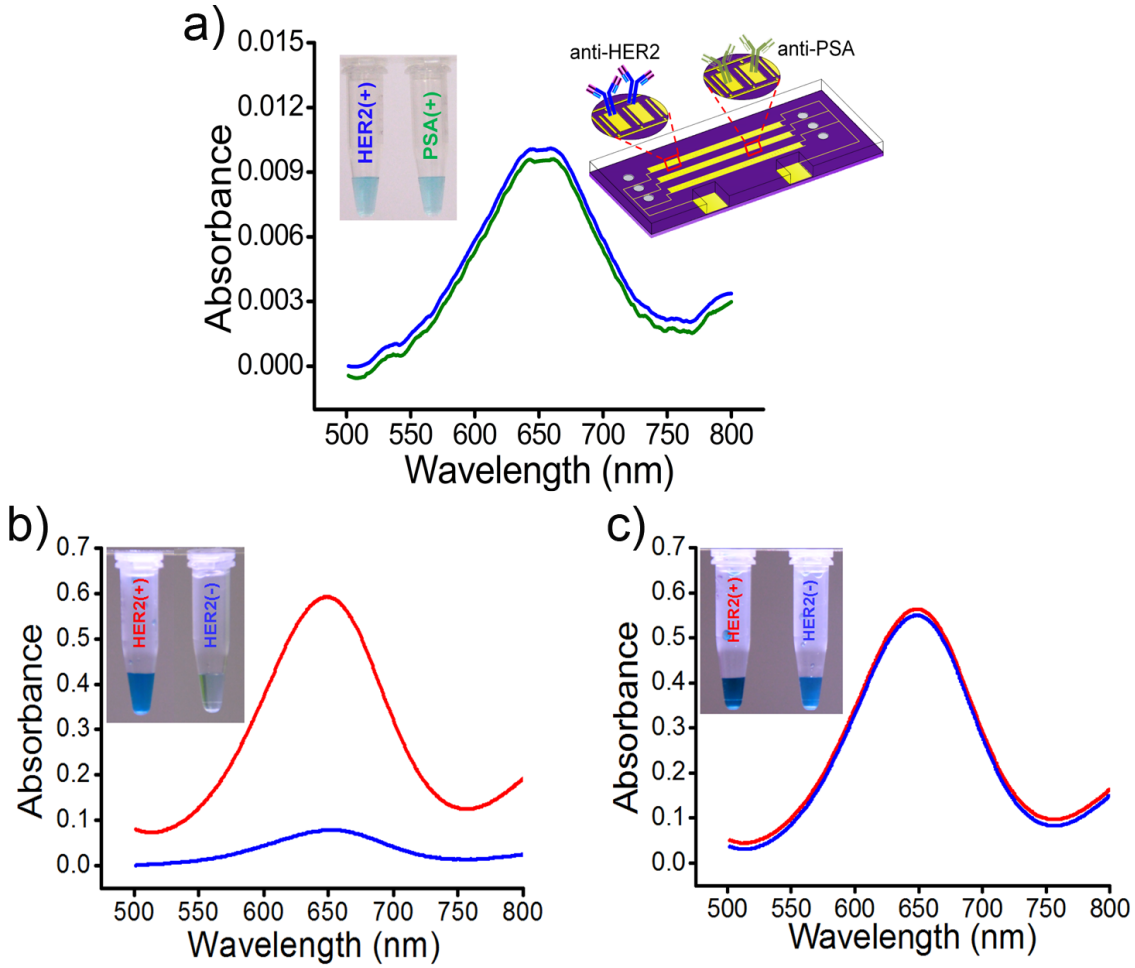
a)
Absorbance
0.015
0.012
0.009
0.006
0.003
0.000
500 550 600 650 700 750 800
Wavelength (nm)
HER2(+)
PSA(+)
anti-HER2
anti-PSA
b)
Absorbance
0.7
0.6
0.5
0.4
0.3
0.2
0.1
0.0
500 550 600 650 700 750 800
Wavelength (nm)
HER2(+)
HER2(-)
c)
Absorbance
0.7
0.6
0.5
0.4
0.3
0.2
0.1
0.0
500 550 600 650 700 750 800
Wavelength (nm)
HER2(+)
HER2(-)

Figure 6.

For TOC only